Veterinary Medicine and Science

WILEY

ORIGINAL ARTICLE OPEN ACCESS

Cats

Construction of a Diagnostic Prediction Model for Feline Nasal and Nasopharyngeal Diseases in Japan Using Noninvasive Examinations

Aki Fujiwara-Igarashi[1] | Yuta Nakazawa[1] | Takafumi Ohshima[1] | Sho Goto[1] | Masatoshi Ino[1] | Yuji Hamamoto[1] | Yoshinori Takeuchi[2] | Hideyuki Kanemoto[3,4]

[1]Laboratory of Veterinary Radiology, School of Veterinary Medicine, Nippon Veterinary and Life Science University, Musashino, Tokyo, Japan | [2]Division of Medical Statistics, Department of Social Medicine, Faculty of Medicine, Toho University, Ota-ku, Tokyo, Japan | [3]DVMs Animal Medical Center Yokohama, Yokohama, Kanagawa, Japan | [4]ER Hachioji Advanced Veterinary Medical Emergency and Critical Care Center, Hachioji, Tokyo, Japan

Correspondence: Aki Fujiwara-Igarashi (afjig@nvlu.ac.jp)

Received: 3 July 2024 | **Revised:** 24 January 2025 | **Accepted:** 7 March 2025

Funding: This study was supported by a KAKENHI grant from the Japan Society for the Promotion of Science (Grant 21K20618) and a grant from the Initiative for Realizing Diversity in the Research Environment from MEXT, Japan (2023–2024).

Keywords: diagnostic prediction model | nasal and nasopharyngeal diseases | nasal and nasopharyngeal tumour | nasopharyngeal stenosis | rhinitis

ABSTRACT

Background: Although feline nasal and nasopharyngeal diseases (NNDs) often require advanced tests under general anaesthesia for definitive diagnosis, not all patients can undergo them.

Objectives: This study aimed to construct diagnostic prediction models for feline NNDs in Japan using noninvasive examinations, signalment and history.

Methods: Seventy-nine cats diagnosed with NNDs, including representative diseases in Japan—nasal and nasopharyngeal tumours (NNT), rhinitis (RS) and nasopharyngeal stenosis (NPS)—were retrospectively investigated to construct prediction models (model group, GM). Thirty-nine cats diagnosed were prospectively investigated to validate their efficacy (validation group, GV). Three predictive models were developed: Models 1 and 2 were manually constructed, with Model 1 designed to predict NNT, RS and NPS individually and Model 2 distinguishing between these diseases. Model 3 was constructed using least absolute shrinkage and selection operator logistic regression. Sensitivity, indicating the ability to identify cases of each disease, and specificity, reflecting the ability to exclude other diseases, were used to assess performance.

Results: In Model 1 of the GV, the sensitivity and specificity for NNT, RS and NPS were 1.00 and 0.73, 0.62 and 0.96 and 0.78 and 0.97, respectively. In Model 2 of the GV, the values were 0.94 and 0.86 for NNT, 0.77 and 0.92 for RS and 0.75 and 0.94 for NPS. In Model 3 of the GV, they were 0.94 and 0.05 for NNT, 0.25 and 1.00 for RS and 0.13 and 0.84 for NPS.

Conclusions: The diagnostic prediction models, particularly Models 1 and 2, could help estimate whether advanced tests are necessary.

1 | Introduction

Among feline nasal and nasopharyngeal diseases (NNDs), neoplasia has been reported to be the most common, whereas other common conditions include acute rhinitis (RS) due to viral infection, chronic rhinitis (CRS), nasopharyngeal stenosis (NPS), inflammatory polyps, foreign bodies and fungal RS (Allen et al. 1999; Fujiwara-Igarashi et al. 2024; Henderson et al. 2004; Reed and Gunn-Moore 2012). Clinical signs, such as nasal discharge, sneezing, reverse sneezing, stertor and epistaxis, are similar

among patients with NNDs (Reed and Gunn-Moore 2012). A study of 75 cats with chronic nasal discharge showed that the aetiologies of NND include neoplasia, fungal RS, lymphocytic-plasmacytic RS and foreign bodies (Demko and Cohn 2007). Radiographic findings in feline nasal diseases have also been reported, and characteristic findings of nasal tumours and CRS have been described (Lamb et al. 2003; O'Brien et al. 1996). According to these reports, displacement of midline structures; invasion of bones and conditions associated with unilateral lesions, such as lysis of the lateral bones, nasal turbinate destruction, loss of teeth and generalized soft tissue opacity, were more frequently detected in cases of nasal tumours than in those of CRS; however, these findings are also observed in CRS. In one report (Lamb et al. 2003), clinical signs were compared between nasal tumour and CRS and epistaxis, sneezing and facial deformities were more common in nasal tumour cases than in CRS cases. However, because these clinical signs can also be observed in CRS, a combination of clinical signs and radiographic findings is needed to assist in diagnoses.

To accurately differentiate between these feline NNDs, advanced imaging tests, such as computed tomography (CT) or magnetic resonance imaging (MRI), rhinoscopy and biopsy under general anaesthesia, are needed. CT findings in various nasal diseases in cats have been reported (Barrs et al. 2014; Beauvois et al. 2023; Bouyssou et al. 2021; Cooley et al. 2022; Lamb et al. 2016; Moreno-Aguado et al. 2020; Oliveira et al. 2012; Reetz et al. 2006; Tromblee et al. 2006). However, not all patients with NNDs can undergo advanced testing because of the risks associated with general anaesthesia, circumstances involving facilities without advanced equipment and owners' financial concerns. Therefore, if cases involving nasal signs can be broadly differentiated based on whether the disease requires advanced tests using noninvasive examinations, including checking for clinical signs, assessing the duration of clinical signs and radiography, cats with NNDs requiring advanced tests could undergo these tests and receive appropriate treatment more quickly.

The construction of diagnostic prediction models for various diseases in veterinary medicine, including Cushing's syndrome (Schofield et al. 2021), intestinal disorders (Basran et al. 2023), hypertrophic cardiomyopathy (Rho et al. 2023), urinary bladder diseases (Jones et al. 2020), acute and chronic kidney diseases (Biourge et al. 2020; Renard et al. 2021) and lymphoma (Haghofer et al. 2023), has been reported; most of these studies used artificial intelligence (AI). Furthermore, we previously reported on diagnostic prediction models for canine nasal diseases (Nakazawa et al. 2023). However, there have been no reports on diagnostic prediction models for feline NNDs. Therefore, the aim of the present study was to retrospectively construct different diagnostic prediction models using noninvasive examinations for feline NND in Japan and to prospectively validate the efficacy of these models.

2 | Materials and Methods

2.1 | Cases

Cats diagnosed with NNDs visiting the Department of Respiratory Medicine, Veterinary Medical Teaching Hospital at Nippon Veterinary and Life Science University (VMTH-NVLU), between August 2013 and April 2021, were retrospectively selected and were included in a diagnostic prediction model (model group, GM). Cats with nasal diseases that visited the VMTH-NVLU and DVMs Animal Medical Center, Yokohama between May 2021 and September 2021 were then prospectively selected to validate the usefulness of the constructed diagnostic prediction model (validation group, GV).

All cats included in the study underwent head radiography and were finally diagnosed using head CT or MRI with contrast enhancement and, if necessary, endoscopy and histopathological examination under general anaesthesia. Patients with epistaxis due to hypertension and thrombocytopenia were excluded through physical or blood examinations; therefore, these patients did not undergo advanced imaging, such as CT and MRI, under general anaesthesia.

Nasal and nasopharyngeal tumours (NNTs) were diagnosed using CT or MRI with heterogeneously enhanced soft tissue findings and histopathological findings acquired via tissue biopsy. CRS was diagnosed on the basis of clinical signs lasting >1 month, CT or MRI findings of basal discharge accumulation, histopathological findings via tissue biopsy and bacterial cultures. Diagnosis of NPS was determined by CT or MRI with stenotic images of the nasopharynx without the surrounding tumours and confirmation by endoscopy. Patients with NPS and concurrent CRS were classified as having NPS. Fungal RS and nasopharyngeal polyps were diagnosed on the basis of CT or MRI findings of heterogeneously enhanced soft tissues and histopathological findings.

Seventy-nine cats were included in the GM. The details regarding the nasal diseases were as follows: NNT (n = 37); RS (n = 26), including CRS (n = 25) and fungal RS due to *Aspergillus* infection (n = 1); NPS (n = 14); nasopharyngeal polyps (n = 1) and nasal stricture due to the brachycephalic breed (n = 1). The GV included 39 cats with the following diseases: NNT (n = 17) and RS (n = 13), all cases of which included cats with CRS; NPS (n = 8) and chronic pharyngitis (n = 1).

2.2 | Candidate Predictors

As candidate predictors, we obtained the cats' breed; sex; age; duration of clinical signs; clinical signs, including nasal discharge (serous, purulent and haemorrhagic), epistaxis, nasal signs (bilateral or unilateral), stertor, sneezing, reverse sneezing, snoring, facial deformity, palate ptosis and mouth breathing and radiographic findings from medical records. Cases with nasal discharge were identified and included one or more of the characteristics. Age was categorized into four groups, <24, 24–71, 72–143 and >143 months, and the duration of clinical signs was categorized into five groups, <1, 1–3, 4–6, 7–12 and >12 months. Radiographic images in two directions with dorsoventral and lateral views were blindly evaluated by two veterinarians (Evaluators 1 and 2). Radiographic findings included increased opacity of the nasal cavity (unilateral or bilateral), left–right difference in the nasal cavity, osteoclasia (nasal turbinate, cribriform, nasal septum, alveolar bone and other bones such as the nasal, maxillary and frontal bones), increased opacity of the

frontal sinus, nasopharyngeal narrowing and nasopharyngeal mass. The left–right difference in the nasal cavity indicated a difference in the degree of opacity in both nasal cavities; therefore, a case of bilateral increased opacity of the nasal cavity was also included. Osteoclasia was defined as the presence of one or more bones, as described above.

2.3 | Construction of Diagnostic Prediction Models and Statistical Analysis

Diagnostic prediction models for feline NNDs were constructed using GM information, and two different methods were employed to construct models with better performance. All patients were categorized into four groups: three based on representative NNDs in Japan, including NNTs, RS, and NPS, and the fourth for all other diseases (Fujiwara-Igarashi et al. 2024).

Using the first method, multiple attempts were made to construct models by manually combining the predictors that were recognized as characteristics of each disease. The model with the best sensitivity and specificity for the three representative NNDs (NNTs, RS and NPS) in Japan was then employed. We attempted to use various types of multi-step conditions and to set the number of conditions, as necessary. This method was used to construct two diagnostic models: one for predicting each of the three diseases individually (Model 1) and another for differentiating the diseases (Model 2). This process was guided by empirical observations and prior knowledge of the clinical and radiographic features associated with these diseases. Specifically, in the case of NNTs, predictors included signalment characteristics, such as middle-to-older age (>6 years); clinical signs, such as facial deformity, palate ptosis, short duration of clinical signs (<7 months) and open-mouth breathing and radiographic findings, including osteoclasia, unilateral increased opacity in the nasal cavity and the presence of a nasopharyngeal mass. For RS, predictors included clinical signs, such as nasal discharge and were characterized by the absence of clinical and radiographic features specific to NNTs and NPS, such as a wide age range, facial deformity, palate ptosis, open-mouth breathing, osteoclasia, unilateral increased opacity in the nasal cavity, nasopharyngeal mass or nasopharyngeal narrowing. For NPS, predictors were based on signalment characteristics, such as younger age (<6 years); clinical signs, such as snoring without nasal discharge or epistaxis and longer duration of clinical signs (>7 months) and radiographic findings of nasopharyngeal narrowing. These were combined, if necessary, with conditions, such as younger age (<2 or <6 years) or clinical sign duration of ≥4 or ≥7 months, to further refine the classification.

Using the second method (Model 3), we applied least absolute shrinkage and selection operator (LASSO) logistic regression to automatically select the predictors for each disease and construct prediction models. We constructed separate models for each disease initially, including the candidate predictors described above with nasal discharge characteristics and osteoclasia types removed. The initial set of candidate predictors included variables, such as breed, sex, age, duration of clinical signs, clinical signs (e.g., nasal discharge, epistaxis and facial deformity) and radiographic findings (e.g., nasopharyngeal narrowing, osteoclasia and increased opacity of the nasal cavity). The optimal values of the tuning parameter for the LASSO logistic regression models were determined by leave-one-out cross-validation. We identified the optimal threshold of the constructed models based on the Youden index (Youden 1950).

The prediction performance of the constructed models was evaluated using GV information. For each model, we calculated sensitivity, which indicates the ability to identify cases of each disease, and specificity, which reflects the ability to exclude other diseases, to assess the model performance in the GV. Additionally, for Model 3, we constructed the receiver operating characteristic (ROC) curve and calculated the *c*-statistics. All statistical analyses were performed using Prism, version 9.00 (GraphPad Software, San Diego, CA) and R version 4.2.3.

3 | Results

3.1 | Case Characteristics

Details of the breed, sex, age, duration of clinical signs, clinical signs, histopathologic type of NNTs and radiographic findings in each group are summarized in Table 1.

Among the 79 cats in the GM group, 37 were diagnosed with NNT, of which lymphoma was the most common disease with 24 cases (65%), followed by adenocarcinoma with eight cases (22%). Non-pedigree cats were the most common breed ($n = 55$), followed by American Shorthair ($n = 3$), Russian Blue ($n = 3$), Somali ($n = 3$), Abyssinian ($n = 2$), Norwegian Forest ($n = 2$), Persian ($n = 2$), Singapore ($n = 2$) and seven pedigree cats with one breed each. Regarding sex, 41 males (38 castrated) and 38 females (37 spayed) were included. The median and mean ages were 114 and 106 months, respectively (range, 5–206).

Among the 39 cats in the GV group, 17 were diagnosed with NNT, of which lymphoma was the most common disease with ten cases (59%), followed by adenocarcinoma with four cases (24%), which was similar to the distribution of NNTs in the GM. Non-pedigree cats were the most common breed ($n = 32$), followed by Russian Blue ($n = 2$) and five pedigree cats with one breed each. Regarding sex, 14 males (13 castrated) and 25 females (18 spayed) were included. The median and mean ages were 122 and 125 months, respectively (range, 5–206).

3.2 | Diagnostic Prediction Models

Model 1 for NNT was defined as meeting one or more of the following five criteria: the presence of facial deformity, the presence of palate ptosis, the presence of osteoclasia on radiographs and duration of clinical signs <7 months, the presence of nasopharyngeal mass on radiographs and duration of clinical signs <7 months and age ≥6 years and duration of clinical signs <7 months. In the GM, the model correctly identified 35 of 37 NNT cases, achieving a sensitivity of 0.95. Among the 42 other NND cases, 35 were correctly excluded, resulting in a specificity of 0.83 (Figure 1). When applied to the GV, the model identified all 17 NNT cases, achieving a sensitivity of 1.00. Among the 22 other NND cases, 6 were misclassified as NNT, resulting in a specificity of 0.73, which was slightly lower than

TABLE 1 | Details of signalment, clinical signs and radiographic findings observed in each nasal disease.

	Nasal and nasopharyngeal tumour ($n = 54$)		Rhinitis ($n = 39$)		Nasopharyngeal stenosis ($n = 22$)		Others ($n = 3$)	
	GM ($n = 37$)	GV ($n = 17$)	GM ($n = 26$)	GV ($n = 13$)	GM ($n = 14$)	GV ($n = 8$)	GM ($n = 2$)	GV ($n = 1$)
	n (%)	*n* (%)	*n* (%)	*n* (%)	*n* (%)	*n* (%)	*n* (%)	*n* (%)
Breed								
Non-pedigree	26 (70)	15 (88)	17 (65)	9 (69)	12 (86)	7 (88)	2 (100)	1 (100)
Pedigree	11 (30)	2 (12)	9 (35)	4 (31)	2 (14)	1 (13)	0 (0)	0 (0)
Sex								
Male	20 (54)	5 (30)	15 (58)	3 (23)	5 (36)	5 (63)	1 (50)	1 (100)
Female	17 (46)	12 (71)	11 (42)	10 (77)	9 (64)	3 (38)	1 (50)	0 (0)
Age								
<24 months	0 (0)	0 (0)	7 (27)	2 (15)	2 (14)	0 (0)	1 (50)	0 (0)
24–71 months	3 (8)	1 (6)	4 (15)	1 (8)	6 (43)	0 (0)	1 (50)	0 (0)
72–143 months	16 (43)	7 (41)	10 (38)	6 (46)	3 (21)	6 (75)	0 (0)	1 (100)
>143 months	18 (49)	9 (53)	5 (19)	4 (31)	3 (21)	2 (25)	0 (0)	0 (0)
Duration of clinical signs								
<1 month	2 (5)	5 (30)	1 (4)	0 (0)	0 (0)	0 (0)	0 (0)	0 (0)
1–3 months	16 (43)	6 (35)	2 (8)	1 (8)	0 (0)	0 (0)	1 (50)	0 (0)
4–6 months	13 (35)	4 (24)	3 (12)	3 (23)	0 (0)	1 (13)	0 (0)	0 (0)
7–12 months	2 (5)	1 (6)	5 (19)	2 (15)	2 (14)	0 (0)	0 (0)	1 (100)
>12 months	4 (11)	1 (6)	15 (58)	7 (54)	12 (86)	7 (88)	1 (50)	0 (0)
Clinical signs								
Palate ptosis	9 (24)	2 (12)	0 (0)	0 (0)	0 (0)	0 (0)	0 (0)	0 (0)
Sneezing	28 (76)	7 (41)	21 (81)	5 (38)	3 (21)	2 (25)	1 (50)	0 (0)
Reverse sneezing	6 (16)	2 (12)	3 (12)	3 (23)	2 (14)	2 (25)	0 (0)	0 (0)
Unilateral nasal signs	14 (38)	10 (59)	11 (42)	5 (38)	1 (7)	2 (25)	0 (0)	0 (0)
Bilateral nasal signs	17 (46)	5 (30)	16 (62)	7 (54)	2 (14)	4 (50)	1 (50)	0 (0)
Nasal discharge	30 (81)	10 (59)	26 (100)	13 (100)	3 (21)	6 (75)	1 (50)	0 (0)
Serous nasal discharge	13 (35)	6 (35)	13 (50)	7 (54)	3 (21)	4 (50)	1 (50)	0 (0)

(Continues)

TABLE 1 | (Continued)

	Nasal and nasopharyngeal tumour ($n = 54$)		Rhinitis ($n = 39$)		Nasopharyngeal stenosis ($n = 22$)		Others ($n = 3$)	
	GM ($n = 37$)	GV ($n = 17$)	GM ($n = 26$)	GV ($n = 13$)	GM ($n = 14$)	GV ($n = 8$)	GM ($n = 2$)	GV ($n = 1$)
	n (%)	*n* (%)	*n* (%)	*n* (%)	*n* (%)	*n* (%)	*n* (%)	*n* (%)
Purulent nasal discharge	23 (62)	7 (41)	19 (73)	8 (62)	2 (14)	3 (38)	1 (50)	0 (0)
Haemorrhagic nasal discharge	19 (51)	7 (41)	15 (58)	5 (38)	0 (0)	2 (25)	1 (50)	0 (0)
Epistaxis	23 (62)	8 (47)	16 (62)	6 (46)	0 (0)	2 (25)	0 (0)	0 (0)
Stertor	34 (92)	9 (53)	24 (92)	8 (62)	13 (93)	8 (100)	2 (100)	1 (100)
Facial deformity	16 (43)	10 (59)	3 (12)	1 (8)	0 (0)	0 (0)	0 (0)	0 (0)
Snoring	16 (43)	5 (29)	10 (38)	7 (54)	11 (79)	6 (75)	2 (100)	0 (0)
Mouth breathing	15 (41)	5 (29)	5 (19)	2 (15)	6 (43)	4 (50)	0 (0)	0 (0)
Radiographical findings								
Unilateral increased opacity	6 (16)	5 (29)	0 (0)	0 (0)	2 (14)	0 (0)	0 (0)	0 (0)
Bilateral increased opacity	26 (70)	10 (59)	23 (88)	11 (85)	7 (50)	4 (50)	1 (50)	0 (0)
Left–right difference	19 (51)	13 (76)	10 (38)	5 (38)	0 (0)	8 (100)	0 (0)	0 (0)
Osteoclasia	27 (73)	15 (88)	19 (73)	9 (69)	6 (43)	6 (75)	1 (50)	0 (0)
Destruction of nasal turbinate	24 (65)	14 (82)	16 (62)	9 (69)	2 (14)	5 (63)	0 (0)	0 (0)
Destruction of cribriform	19 (51)	9 (53)	9 (35)	5 (38)	6 (43)	2 (25)	1 (50)	0 (0)
Destruction of nasal septum	7 (19)	2 (12)	3 (12)	3 (23)	1 (7)	0 (0)	0 (0)	0 (0)
Destruction of alveolar bone	1 (3)	1 (6)	2 (8)	1 (8)	2 (14)	0 (0)	0 (0)	0 (0)
Destruction of other bone (nasal, maxillary and frontal bones)	3 (8)	6 (35)	3 (12)	1 (8)	0 (0)	0 (0)	0 (0)	0 (0)
Increased opacity of frontal sinus	29 (78)	14 (82)	23 (88)	9 (69)	9 (64)	2 (25)	0 (0)	0 (0)
Nasopharyngeal narrowing	0 (0)	0 (0)	0 (0)	1 (8)	7 (50)	6 (75)	0 (0)	0 (0)
Nasopharyngeal mass	12 (32)	2 (12)	0 (0)	0 (0)	1 (7)	1 (13)	1 (50)	0 (0)

Abbreviations: GM, model group; GV, validation group.

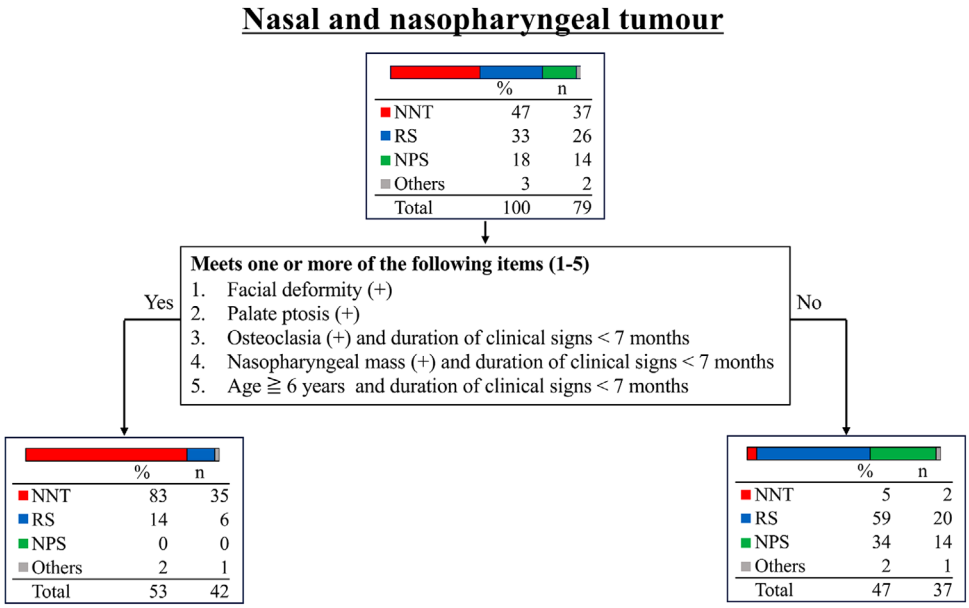

FIGURE 1 | Diagnostic prediction steps for NNTs using a manually constructed model (Model 1). The bar graph illustrates the proportion of patients with each disease in the model group. NNT, nasal and nasopharyngeal tumour; NPS, nasopharyngeal stenosis; RS, rhinitis.

TABLE 2 | Sensitivity and specificity in diagnostic prediction models.

		GM		GV	
		Sensitivity	**Specificity**	**Sensitivity**	**Specificity**
Model 1	Nasal and nasopharyngeal tumour	0.95	0.83	1.00	0.73
	Rhinitis	0.85	0.91	0.62	0.96
	Nasopharyngeal stenosis	0.86	1.00	0.75	0.94
Model 2	Nasal and nasopharyngeal tumour	0.84	0.88	0.94	0.86
	Rhinitis	0.85	0.85	0.77	0.92
	Nasopharyngeal stenosis	0.79	0.97	0.75	0.94
Model 3	Nasal and nasopharyngeal tumour	1.00	0.83	0.94	0.05
	Rhinitis	0.85	0.96	0.25	1.00
	Nasopharyngeal stenosis	1.00	1.00	0.13	0.84

Abbreviations: GM, model group; GV, validation group.

that in the GM (Table 2). The first condition of Model 1 for RS was defined as meeting the following criteria: the presence of nasal discharge, the absence of palate ptosis, the absence of nasopharyngeal narrowing on radiographs and the absence of nasopharyngeal mass on radiographs. Patients that met these conditions proceeded to the second condition: those aged <2 years. Next, patients that did not meet the second condition proceeded to the third condition, which was meeting one or more of the following criteria: the presence of facial deformity, the presence of osteoclasia on radiographs and duration of clinical signs <4 months and age ≥6 years and duration of clinical signs <7 months. Finally, cases that met the second condition and those that did not meet the third condition were defined as positive for RS in Model 1 (Figure 2). In the GM, the model correctly identified 22 of 26 RS cases, resulting in a sensitivity of 0.85 and excluded 48 of 53 other NND cases, yielding a specificity of 0.91. When applied to the GV, the model identified 8 of 13 RS cases, resulting in a lower sensitivity of 0.62, while correctly excluding 25 of 26 other NND cases, achieving a specificity of 0.96, comparable to the high specificity observed in the GM (Table 2). Finally, Model 1 for NPS included two conditions. The first condition was nasopharyngeal narrowing observed on radiography. Cases which did not meet the criterion for the first condition proceeded to the second condition by meeting all the following criteria: the absence of nasal discharge, the absence of epistaxis and the duration of clinical signs ≥7 months. Finally, cases which met the criterion for the first condition and cases which met the criterion for the second condition were defined as positive for NPS in Model 1 (Figure 3). In the GM, the model correctly identified 12 of 14 NPS cases, resulting in a sensitivity of 0.86 and excluded all 65 other NND cases, yielding a specificity of 1.00. When applied to the GV, the model identified 6 of 8 NPS cases, resulting in a slightly lower sensitivity of 0.75, while correctly excluding 29 of 31 other NND cases, achieving a specificity of

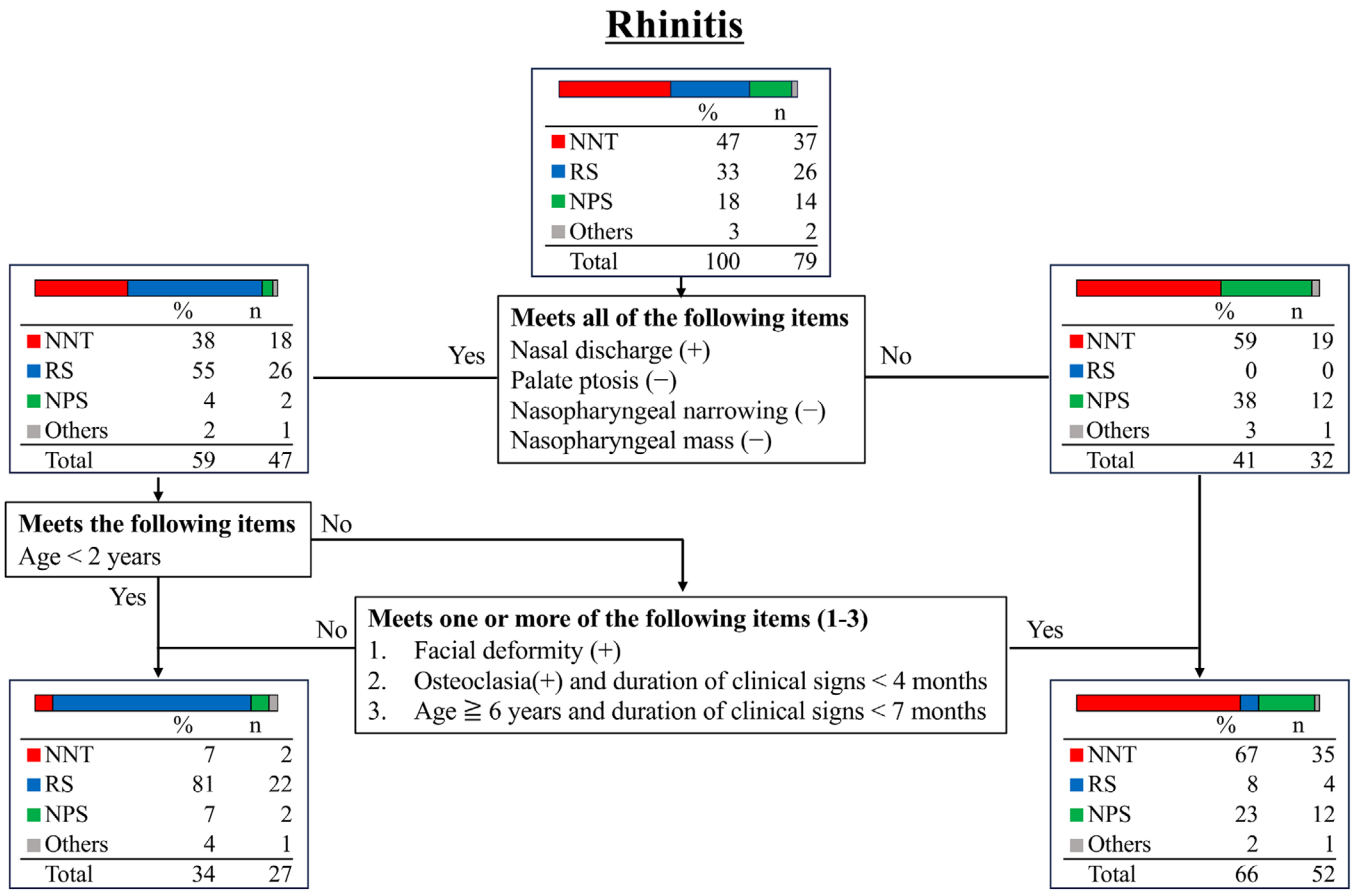

FIGURE 2 | Diagnostic prediction steps for RS using a manually constructed model (Model 1). The bar graph illustrates the proportion of patients with each disease in the model group. NNT, nasal and nasopharyngeal tumour; NPS, nasopharyngeal stenosis; RS, rhinitis.

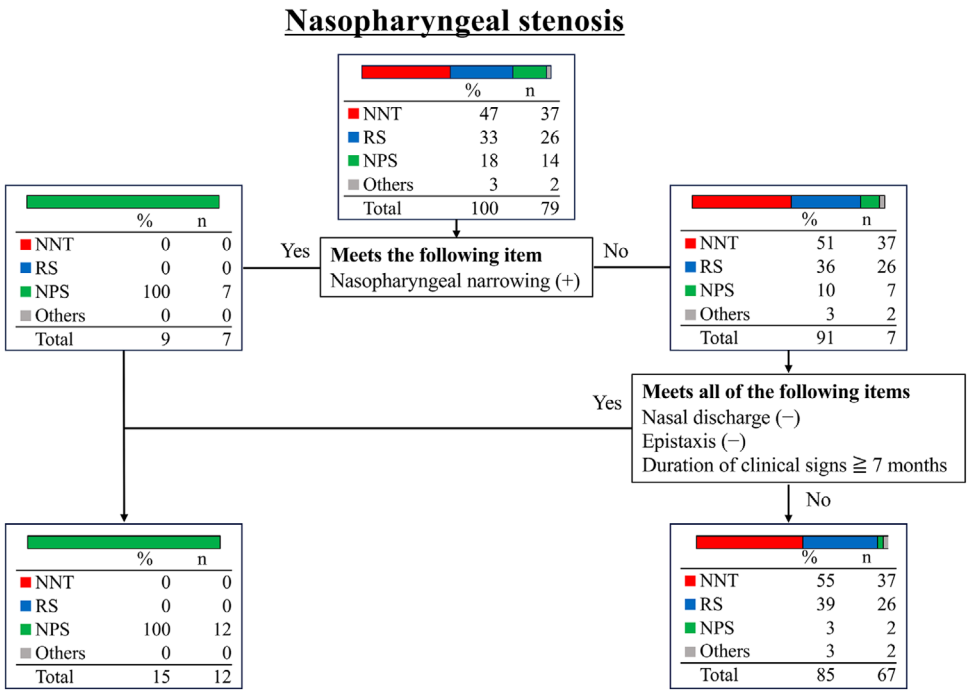

FIGURE 3 | Diagnostic prediction steps for NPS using a manually constructed model (Model 1). The bar graph illustrates the proportion of patients with each disease in the model group. NNT, nasal and nasopharyngeal tumour; NPS, nasopharyngeal stenosis; RS, rhinitis.

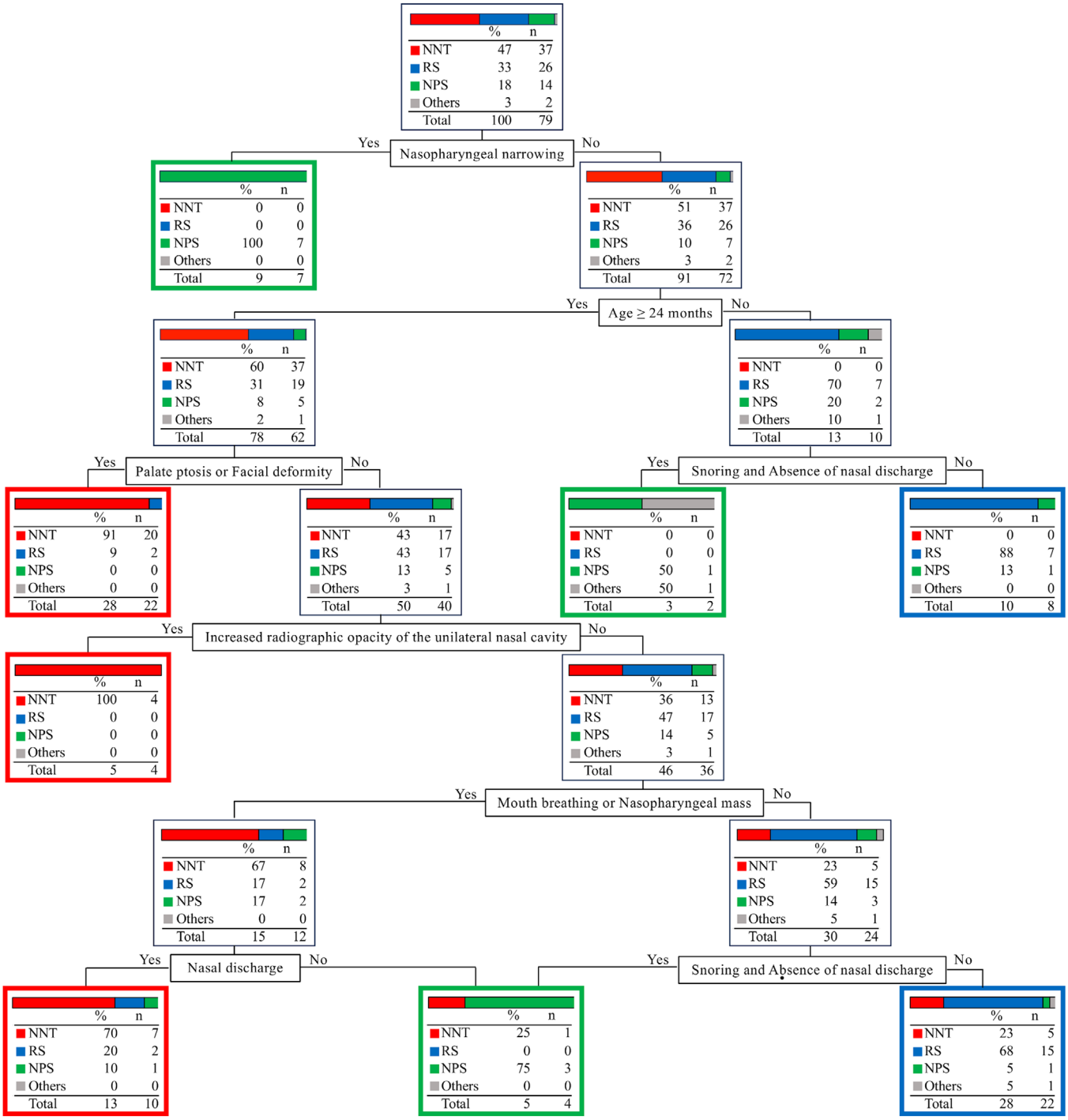

FIGURE 4 | Diagnostic prediction steps for distinguishing among NNTs, RS and NPS using a manually constructed model (Model 2). The cases were classified into three diseases, with each disease represented by the colour of the nodes at the end of each branch: red nodes for NNT, blue nodes for RS and green nodes for NPS. The bar graph illustrates the proportion of patients with each disease in the model group. NNT, nasal and nasopharyngeal tumour; NPS, nasopharyngeal stenosis; RS, rhinitis.

0.94, which was similarly high to that observed in the GM (Table 2).

Model 2 was constructed with multi-layered classification, effectively differentiating among NNT, RS and NPS using various diagnostic items (Figure 4). Regarding signalment, age was considered, specifically focusing on whether the cat was ≥24 months old. Clinical signs used for differentiation include nasal discharge, snoring, palate ptosis, facial deformity and mouth breathing. Radiographic findings consisted of nasopharyngeal narrowing, increased radiographic opacity of the unilateral nasal cavity and the presence of a nasopharyngeal mass. Among the models in the GM, Model 2 successfully classified 31 of 37 cases of NNT, resulting in a sensitivity of 0.84, while correctly excluding 37 of 42 other NND cases, achieving a specificity of 0.88. For RS, the model identified 22 of 26 cases of RS, with a sensitivity of

TABLE 3 | Details of prediction models constructed using least absolute shrinkage and selection operator logistic regression (Model 3).

	Variables	Coefficient	*c*-statistic	Optimal cut-off value
Nasal and nasopharyngeal tumour	Intercept	0.023		
	Age >143 months	0.23	GM: 0.98 GV: 0.38	0.36
	Duration of clinical signs <4 months	0.18		
	Palate ptosis	0.32		
	Facial deformity	0.73		
	Left–right difference	0.14		
	Nasopharyngeal mass	0.26		
Rhinitis	Intercept	−1.6		
	Age >143 months	0.10	GM: 0.97 GV: 0.80	0.49
	Duration of clinical signs >12 months	0.13		
	Nasal discharge	1.65		
Nasopharyngeal stenosis	Intercept	−0.87		
	Duration of clinical signs >12 months	0.91	GM: 1.00 GV: 0.36	0.41
	Nasopharyngeal narrowing	1.90		

Abbreviations: GM, model group; GV, validation group.

0.85 and excluded 45 of 53 other NND cases, yielding a specificity of 0.85. Similarly, for NPS, the model identified 11 of 14 cases, achieving a sensitivity of 0.79 and correctly excluded 63 of 65 other NND cases, resulting in a specificity of 0.97. When applied to the GV, the model correctly identified 16 of 17 NNT cases, achieving a sensitivity of 0.94, while excluding 19 of 22 other NND cases, resulting in a specificity of 0.86. For RS, 10 of 13 cases were correctly identified, corresponding to a sensitivity of 0.77, and 24 of 26 other NND cases were excluded, achieving a specificity of 0.92. For NPS, the model classified 6 of 8 cases correctly, resulting in a sensitivity of 0.75 while excluding 29 of 31 other NND cases, yielding a specificity of 0.94. These findings demonstrate that although sensitivity for RS was slightly lower in the GV, sensitivity and specificity for each disease (NNT, RS and NPS) in the GV were maintained at similarly high values to those in the GM, indicating that the models reliably differentiated between these diseases based on the selected predictors (Table 2).

In the construction of Model 3 using the GM, variables were selected, and the log-odds ratio for the variables was calculated using LASSO logistic regression analysis. The coefficient values and ROC curve of Model 3 for each disease are shown in Table 3 and Figure 5, respectively. Model 3 for NNT included (i.e., coefficient ≠ 0) age >143 months, duration of clinical signs <4 months, the presence of palate ptosis, the presence of facial deformity, left–right difference on radiographs and nasopharyngeal mass on radiographs (Table 3). The *c*-statistic value, sensitivity and specificity were 0.98, 1.00 and 0.83, respectively. The optimal cut-off value of 0.36 was determined on the basis of the Youden index. However, when fitting the model to the GV, the model's performance decreased, with a *c*-statistic of 0.38, sensitivity of 0.94 and specificity of 0.05 (Tables 2 and 3). For RS, the model included age >143 months, duration of clinical signs >12 months and the presence of nasal discharge (Table 3). The *c*-statistic value, sensitivity and specificity were 0.97, 0.85 and 0.96, respectively, at the optimal cut-off value of 0.49. When we fitted the model to the GV, the *c*-statistic decreased to 0.80, and specificity remained at 1.00, whereas sensitivity was markedly lower at 0.25 (Tables 2 and 3). For NPS, the model included duration of clinical signs >12 months and nasopharyngeal narrowing on radiographs (Table 3). The *c*-statistic value, sensitivity and specificity were 1.00, 1.00 and 1.00 at the optimal cut-off value of 0.41. On fitting the model to the GV, the *c*-statistic decreased to 0.36, and specificity remained relatively high at 0.84, whereas sensitivity was notably lower at 0.13 (Tables 2 and 3).

4 | Discussion

A total of 77 and 39 cats were included in the GM and GV, respectively. To construct diagnostic prediction models for feline NNDs, including NNT, RS and NPS, different methods were employed, such as the construction of Models 1, 2 and 3 using GM information. GV information was used to validate their efficacy. The trends in the NNDs were similar in both the GM and GV, particularly when using Models 1 and 2.

Regarding age, 50 of the 54 patients were over 6 years of age, and characteristic results were obtained in the NNT group. In contrast, 25 of the 39 patients with RS and 14 of the 22 patients with NPS were aged >6 years; therefore, age was not strongly associated with these diseases. In the NNT group, the median age

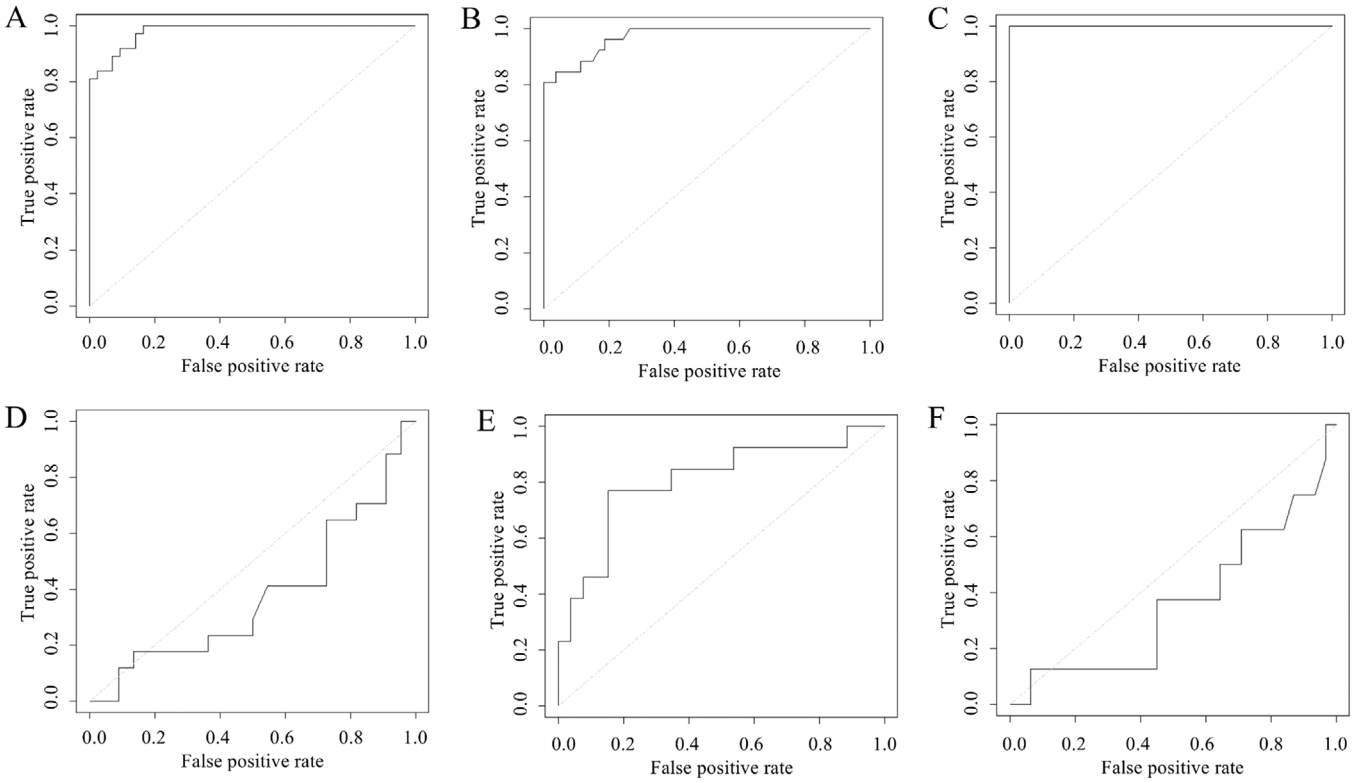

FIGURE 5 | ROC curves for Model 3. (A) NNT in GM: *c*-statistic = 0.98, (B) RS in GM: *c*-statistic = 0.97, (C) NPS in GM: *c*-statistic = 1.0, (D) NNT in GV: *c*-statistic = 0.38, (E) RS in GV: *c*-statistic = 0.80 and (F) NPS in GV: *c*-statistic = 0.36. GM, model group; GV, validation group; NNT, nasal and nasopharyngeal tumour; NPS, nasopharyngeal stenosis; ROC, receiver operating characteristic; RS, rhinitis.

of patients with nasal lymphoma was reported to be 8.4–11 years, and patients as young as 1–2 years old were included (Fujiwara-Igarashi et al. 2014; Goto et al. 2022; Haney et al. 2009; Nakazawa et al. 2021). The median age of patients with NNTs, except for nasal lymphoma, was 11.8–13.3 years old (Fujiwara-Igarashi et al. 2014; Giuliano and Dobson 2020; Stiborova et al. 2020; Yoshikawa et al. 2021). On performing comparisons among histopathological types, lymphoma tended to occur in younger patients than those with other histopathological types. However, the diagnostic model for NNT was constructed using all histopathological types in this study owing to the limited number of cases. Conversely, RS has been reported in patients of various ages, with a median age of 4.3 years (Johnson et al. 2005; Michiels et al. 2016). As for NPS, the median age of patients has been reported to be 3.0–4.0 years old (Burdick et al. 2018; De Lorenzi et al. 2016). Therefore, our results regarding age aligned with those of previous studies.

As for clinical signs, a remarkable trend was observed in their duration. Clinical signs for <7 months occurred in 46 of the 54 cases with NNT; in RS and NPS, the duration was ≥7 months in 29 of the 39 cases and 21 of the 22 cases, respectively. In the NPS group, stertor ($n = 21$, 95.5%) and snoring ($n = 17$, 77.2%) were the most common clinical signs, and nasal discharge was not always observed ($n = 9$, 40.9%). Nasal discharge may have been caused by the concurrence of CRS or poor drainage due to nasopharyngeal obstruction. Stertor has been observed in all NPS cases in previous reports and, in some cases, has been reported to be concurrent with CRS (Burdick et al. 2018; De Lorenzi et al. 2016). Palate ptosis and facial deformity were most frequently observed in NNT; all patients with palate ptosis had NNT, and 26 of the 30 patients with facial deformity had NNT. Therefore, palatal ptosis and facial deformities may be specific to NNT. Nasal discharge was not associated with NNT; epistaxis and haemorrhagic nasal discharge were observed not only in NNT but also in RS.

Regarding radiographic findings, nasopharyngeal narrowing was the sole characteristic finding in NPS. Dorsal deviation or deformation of the caudal part of the soft palate has been reported as a radiographic finding in NPS (De Lorenzi et al. 2016), and our results support these findings. A nasopharyngeal mass is also a characteristic finding in NNT. Other radiographic findings have also been detected in some types of nasal diseases. Although osteoclasia was observed in the NNT ($n = 42$) and RS ($n = 28$) groups, different trends were observed between them. In NNT, osteoclasia can occur in various regions of the nasal cavity, and left–right differences are more common than in RS (59.3% and 38.5%, respectively). Although NNT and RS have their own radiographic characteristics, many findings were observed in both diseases, as previously reported (Lamb et al. 2003; O'Brien et al. 1996).

We constructed diagnostic prediction models using different methods and found that the sensitivity and specificity of Models 1 and 2 were superior to those of Model 3. Although the variables used among these models were similar, setting conditions that combined multiple items and classifications using multiple steps in Models 1 and 2 may have been associated with favourable results. Although the *c*-statistics computed using the GM for all Models 3 were very close to one, these statistics exhibited a decline upon evaluation using the GV. This indicates that the

regression models constructed via LASSO were still likely affected by overfitting, probably due to a very small number of cases. Furthermore, this may be due in part to the fact that some variables followed a trend among feline NNDs. However, these models were constructed using a total of 77 and 39 cats in the GM and GV, respectively; therefore, these models, especially Models 1 and 2, may be useful for the differentiation of feline NNDs.

This study had some limitations. The study included a relatively small sample size (GM: $n = 79$, GV: $n = 39$), which may affect the generalizability of our findings. This limitation likely contributed to the overfitting observed in the construction of Model 3, as shown by the decline in *c*-statistics when applied to the GV. Additionally, there was bias in the distribution of diseases because the institutions where the present study was conducted are secondary hospitals. Patients with acute RS caused by viral infections were not included in this study. This disease is common in juvenile cats living outside and in groups living in shelters (Thiry et al. 2009). RS is most commonly acute; therefore, patients with acute RS cannot visit a secondary hospital. The number of fungal RS cases was also limited, and only one case of *Aspergillus* infection was included. Although the frequency of fungal RS in cats is unclear, the fact that our institutes were located in metropolitan areas in Japan may have contributed to its low occurrence. Cryptococcus and *Aspergillus* infections are widely known to cause fungal RS in cats and the radiographic findings in the soft tissues in the nasal cavity and nasopharynx resemble those in NNT (Barrs et al. 2020; Cooley et al. 2022; Karnik et al. 2009). Therefore, to construct a diagnostic model for fungal RS, clinical signs and disease duration should be fully considered. Other types of RS include those caused by foreign bodies and dental diseases. Both these types of RS occur infrequently; therefore, further studies are needed to construct more detailed models of RS based on the cause. Furthermore, patients with nasal diseases were divided into an 'others' group that included conditions, such as nasopharyngeal polyps, nasal strictures due to brachycephalic breed and chronic pharyngitis, similar to in previous studies (Anagrius et al. 2021; Berns et al. 2020; Lamb et al. 2016; Oliveira et al. 2012; Sieslack et al. 2021; White et al. 1992); however, diagnostic prediction models could not be constructed for these other conditions owing to the limited numbers of cases. For nasopharyngeal polyps, radiographic findings, such as nasopharyngeal masses, are considered to be similar to those seen in NNT; therefore, various items must be combined to construct diagnostic prediction models. Future studies should include larger and more diverse cohorts to improve the generalizability and robustness of the diagnostic prediction models proposed in this study. Increasing the sample size will allow for better differentiation of rarer conditions, such as fungal RS and nasopharyngeal polyps, and enhance the accuracy of these models. Particularly, incorporating data from a broader range of clinical institutions, including primary care clinics, may help further refine the models. Regarding other limitations, it is necessary to accurately evaluate radiographs using these prediction models. In this study, radiographic images were evaluated by veterinarians with expertise in respiratory medicine. Although AI may be one way to accurately diagnose radiographic images, there have not yet been any reports for NND, although AI-based radiographical diagnosis focusing on the chest has been recently reported (Boissady et al. 2020; Dumortier et al. 2022; Tahghighi et al. 2023; Yoon et al. 2019). At present, it would be essential that radiographs deemed worthy of evaluation be assessed by radiology specialists with expertise in respiratory medicine when using the prediction models from this study.

5 | Conclusion

Our diagnostic prediction models were constructed for three frequently occurring nasal diseases in cats. Although there were some limitations in terms of them not covering other nasal diseases whose occurrence is rare, this is the first report on the construction of diagnostic prediction models for feline NNDs. The use of the prediction models of the present study could serve to estimate whether advanced imaging tests performed under general anaesthesia are necessary for rapid and appropriate diagnosis and treatment, especially in cats with NNT and NPS.

Author Contributions

Aki Fujiwara-Igarashi: conceptualization, data curation, formal analysis, funding acquisition, investigation, project administration, resources, supervision, visualization, writing – original draft, writing – review and editing. **Yuta Nakazawa**: investigation, project administration, resources. **Takafumi Ohshima**: data curation. **Sho Goto**: data curation, formal analysis, visualization and writing. **Masatoshi Ino**: data curation. **Yuji Hamamoto**: resources. **Yoshinori Takeuchi**: methodology and formal analysis. **Hideyuki Kanemoto**: data curation and resources.

Acknowledgements

We thank Dr. Yui Tomo, Keio University School of Medicine for the advice on statistical methods.

Ethics Statement

The authors confirm that the ethical policies of the journal, as noted on the journal's author guidelines page, have been adhered to.

Consent

Written informed consent for data collection was obtained from the owners of each cat.

Conflicts of Interest

The authors declare no conflicts of interest.

Data Availability Statement

The data that support the findings of this study are available from the corresponding author upon reasonable request.

Peer Review

The peer review history for this article is available at https://www.webofscience.com/api/gateway/wos/peer-review/10.1002/vms3.70296.

References

Allen, H. S., J. Broussard, K. Noone, and G. Allen. 1999. "Nasopharyngeal Diseases in Cats: A Retrospective Study of 53 Cases (1991-1998)." *Journal of the American Animal Hospital Association* 35: 457–461.

Anagrius, K. L., M. Dimopoulou, A. N. Moe, A. Petterson, and I. Ljungvall. 2021. "Facial Conformation Characteristics in Persian and Exotic Shorthair Cats." *Journal of Feline Medicine and Surgery* 23: 1089–1097.

Barrs, V. R., J. J. Talbot, and J. Smith. 2020. "Fungal Rhinosinusitis and Disseminated Invasive Aspergillosis in Cats." *Veterinary Clinics of North America* 50: 331–357.

Barrs, V. R., J. A. Beatty, N. K. Dhand, et al. 2014. "Computed Tomographic Features of Feline Sino-Nasal and Sino-Orbital Aspergillosis." *Veterinary Journal* 201: 215–222.

Basran, P. S., N. Shcherban, M. Forman, et al. 2023. "Combining Ultrasound Radiomics, Complete Blood Count, and Serum Biochemical Biomarkers for Diagnosing Intestinal Disorders in Cats Using Machine Learning." *Veterinary Radiology and Ultrasound* 64: 890–903.

Beauvois, M., P. Colombe, A. M. Canonne, and J. Mortier. 2023. "Cats With Idiopathic Chronic Rhinosinusitis That Develop Clinical Signs Before Two Years of Age Have More Severe Nasal Conchal Lysis, Sinus Malformation, and More Severe Inflammation on Histological Examination." *Journal of the American Veterinary Medical Association* 261: 1481–1487.

Berns, C. N., C. W. Schmiedt, V. M. Dickerson, and S. M. Murphy. 2020. "Single Pedicle Advancement Flap for Treatment of Feline Stenotic Nares: Technique and Results in Five Cases." *Journal of Feline Medicine and Surgery* 22: 1238–1242.

Biourge, V., S. Delmotte, A. Feugier, R. Bradley, M. McAllister, and J. Elliott. 2020. "An Artificial Neural Network-Based Model to Predict Chronic Kidney Disease in Aged Cats." *Journal of Veterinary Internal Medicine* 34: 1920–1931.

Boissady, E., A. de La Comble, X. Zhu, and A. M. Hespel. 2020. "Artificial Intelligence Evaluating Primary Thoracic Lesions Has an Overall Lower Error Rate Compared to Veterinarians or Veterinarians in Conjunction With the Artificial Intelligence." *Veterinary Radiology and Ultrasound* 61: 619–627.

Bouyssou, S., G. J. Hammond, and C. Eivers. 2021. "Comparison of CT Features of 79 Cats With Intranasal Mass Lesions." *Journal of Feline Medicine and Surgery* 23: 987–995.

Burdick, S., A. C. Berent, C. Weisse, et al. 2018. "Interventional Treatment of Benign Nasopharyngeal Stenosis and Imperforate Nasopharynx in Dogs and Cats: 46 Cases (2005-2013)." *Journal of the American Veterinary Medical Association* 253: 1300–1308.

Cooley, S., G. Galustanian, A. Moon, and S. Summers. 2022. "CT Findings of Nasal Cryptococcosis in Cats and Dogs: A Case Series." *Veterinary Radiology and Ultrasound* 63: 422–429.

De Lorenzi, D., D. Bertoncello, S. Comastri, and E. Bottero. 2016. "Treatment of Acquired Nasopharyngeal Stenosis Using a Removable Silicone Stent." *Journal of Feline Medicine and Surgery* 17: 117–124.

Demko, J. L., and L. A. Cohn. 2007. "Chronic Nasal Discharge in Cats: 75 Cases (1993-2004)." *Journal of the American Veterinary Medical Association* 230: 1032–1037.

Dumortier, L., F. Guépin, M. L. Delignette-Muller, C. Boulocher, and T. Grenier. 2022. "Deep Learning in Veterinary Medicine, an Approach Based on CNN to Detect Pulmonary Abnormalities From Lateral Thoracic Radiographs in Cats." *Scientific Reports* 12: 11418.

Fujiwara-Igarashi, A., T. Fujimori, M. Oka, et al. 2014. "Evaluation of Outcomes and Radiation Complications in 65 Cats With Nasal Tumours Treated With Palliative Hypofractionated Radiotherapy." *Veterinary Journal* 202: 455–461.

Fujiwara-Igarashi, A., T. Ohshima, R. Kojima, M. Fujita, and Y. Nakazawa. 2024. "Retrospective Study of 540 Cats With Respiratory Diseases in Japan (2003-2020)." *Veterinary Medical Science* 10: e1456.

Giuliano, A., and J. Dobson. 2020. "Clinical Response and Survival Time of Cats With Carcinoma of the Nasal Cavity Treated With Palliative Coarse Fractionated Radiotherapy." *Journal of Feline Medicine and Surgery* 22: 922–927.

Goto, S., R. Iwasaki, H. Sakai, and T. Mori. 2022. "Combined Hypofractionated Radiotherapy and Chemotherapy Versus Hypofractionated Radiotherapy Alone for Cats With Localized Sinonasal Lymphoma." *Journal of the American Animal Hospital Association* 58: 254–261.

Haghofer, A., A. Fuchs-Baumgartinger, K. Lipnik, et al. 2023. "Histological Classification of Canine and Feline Lymphoma Using a Modular Approach Based on Deep Learning and Advanced Image Processing." *Scientific Reports* 13: 19436.

Haney, S. M., L. Beaver, J. Turrel, et al. 2009. "Survival Analysis of 97 Cats With Nasal Lymphoma: A Multi-Institutional Retrospective Study (1986-2006)." *Journal of Veterinary Internal Medicine* 23: 287–294.

Henderson, S. M., K. Bradley, M. J. Day, et al. 2004. "Investigation of Nasal Disease in the Cat—A Retrospective Study of 77 Cases." *Journal of Feline Medicine and Surgery* 6: 245–257.

Johnson, L. R., J. E. Foley, H. E. De Cock, H. E. Clarke, and D. J. Maggs. 2005. "Assessment of Infectious Organisms Associated With Chronic Rhinosinusitis in Cats." *Journal of the American Veterinary Medical Association* 227: 579–585.

Jones, E., J. Alawneh, M. Thompson, C. Palmieri, K. Jackson, and R. Allavena. 2020. "Predicting Diagnosis of Australian Canine and Feline Urinary Bladder Disease Based on Histologic Features." *Veterinary Sciences* 7: 190.

Karnik, K., J. K. Reichle, A. J. Fischetti, and J. M. Goggin. 2009. "Computed Tomographic Findings of Fungal Rhinitis and Sinusitis in Cats." *Veterinary Radiology and Ultrasound* 50: 65–68.

Lamb, C. R., S. Richbell, and P. Mantis. 2003. "Radiographic Signs in Cats With Nasal Disease." *Journal of Feline Medicine and Surgery* 5: 227–235.

Lamb, C. R., K. Sibbing, and S. L. Priestnall. 2016. "Pathologic Basis for Rim Enhancement Observed in Computed Tomographic Images of Feline Nasopharyngeal Polyps." *Veterinary Radiology and Ultrasound* 57: 130–136.

Michiels, L., M. J. Day, F. Snaps, P. Hansen, and C. Clercx. 2016. "A Retrospective Study of Non-Specific Rhinitis in 22 Cats and the Value of Nasal Cytology and Histopathology." *Journal of Feline Medicine and Surgery* 5: 279–285.

Moreno-Aguado, B., I. Carrera, A. Holdsworth, P. Agthe, T. W. Maddox, and T. Trevail. 2020. "CT Findings in 20 Dogs and Six Cats With Confirmed Nasal Foreign Bodies." *Veterinary Radiology and Ultrasound* 61: 417–426.

Nakazawa, M., H. Tomiyasu, K. Suzuki, et al. 2021. "Efficacy of Chemotherapy and Palliative Hypofractionated Radiotherapy for Cats With Nasal Lymphoma." *Journal of Veterinary Medical Science* 83: 456–460.

Nakazawa, Y., T. Ohshima, H. Kanemoto, and A. Fujiwara-Igarashi. 2023. "Construction of Diagnostic Prediction Model for Canine Nasal Diseases Using Less Invasive Examinations Without Anesthesia." *Journal of Veterinary Medical Science* 85: 1083–1093.

O'Brien, R. T., S. M. Evans, J. A. Wortman, and M. J. Hendrick. 1996. "Radiographic Findings in Cats With Intranasal Neoplasia or Chronic Rhinitis: 29 Cases (1982-1988)." *Journal of the American Veterinary Medical Association* 208: 385–389.

Oliveira, C. R., R. T. O'Brien, J. S. Matheson, and I. Carrera. 2012. "Computed Tomographic Features of Feline Nasopharyngeal Polyps." *Veterinary Radiology and Ultrasound* 53: 406–411.

Reed, N., and D. Gunn-Moore. 2012. "Nasopharyngeal Disease in Cats: 1. Diagnostic Investigation." *Journal of Feline Medicine and Surgery* 14: 306–315.

Reetz, J. A., W. Maï, K. B. Muravnick, M. H. Goldschmidt, and T. Schwarz. 2006. "Computed Tomographic Evaluation of Anatomic and Pathologic Variations in the Feline Nasal Septum and Paranasal Sinuses." *Veterinary Radiology and Ultrasound* 47: 321–327.

Renard, J., M. R. Faucher, A. Combes, D. Concordet, and B. S. Reynolds. 2021. "Machine-Learning Algorithm as a Prognostic Tool in Non-Obstructive Acute-on-Chronic Kidney Disease in the Cat." *Journal of Feline Medicine and Surgery* 23: 1140–1148.

Rho, J., S. M. Shin, K. Jhang, et al. 2023. "Deep Learning-Based Diagnosis of Feline Hypertrophic Cardiomyopathy." *PLoS ONE* 18: e0280438.

Schofield, I., D. C. Brodbelt, N. Kennedy, et al. 2021. "Machine-Learning Based Prediction of Cushing's Syndrome in Dogs Attending UK Primary-Care Veterinary Practice." *Scientific Reports* 11: 9035.

Sieslack, J., D. Farke, K. Failing, M. Kramer, and M. J. Schmidt. 2021. "Correlation of Brachycephaly Grade With Level of Exophthalmos, Reduced Airway Passages and Degree of Dental Malalignment in Persian Cats." *PLoS ONE* 16: e0254420.

Stiborova, K., V. S. Meier, M. Takada, et al. 2020. "Definitive-Intent Radiotherapy for Sinonasal Carcinoma in Cats: A Multicenter Retrospective Assessment." *Veterinary and Comparative Oncology* 18: 626–633.

Tahghighi, P., R. B. Appleby, N. Norena, E. Ukwatta, and A. Komeili. 2023. "Machine Learning Can Appropriately Classify the Collimation of Ventrodorsal and Dorsoventral Thoracic Radiographic Images of Dogs and Cats." *American Journal of Veterinary Research* 84: ajvr23030062.

Thiry, E., D. Addie, S. Belák, et al. 2009. "Feline Herpesvirus Infection. ABCD Guidelines on Prevention and Management." *Journal of Feline Medicine and Surgery* 11: 547–555.

Tromblee, T. C., J. C. Jones, A. E. Etue, and S. D. Forrester. 2006. "Association Between Clinical Characteristics, Computed Tomography Characteristics, and Histologic Diagnosis for Cats With Sinonasal Disease." *Veterinary Radiology and Ultrasound* 47: 241–248.

White, S. D., R. A. Rosychuk, T. A. Janik, P. Denerolle, and P. Schultheiss. 1992. "Plasma Cell Stomatitis-Pharyngitis in Cats: 40 Cases (1973-1991)." *Journal of the American Veterinary Medical Association* 200: 1377–1380.

Yoon, Y., T. Hwang, H. Choi, and H. Lee. 2019. "Classification of Radiographic Lung Pattern Based on Texture Analysis and Machine Learning." *Journal of Veterinary Science* 20: e44.

Yoshikawa, H., T. L. Gieger, C. F. Saba, et al. 2021. "Retrospective Evaluation of Intranasal Carcinomas in Cats Treated With External-Beam Radiotherapy: 42 Cases." *Journal of Veterinary Internal Medicine* 35: 1018–1030.

Youden, W. J. 1950. "Index for Rating Diagnostic Tests." *Cancer* 3: 32–35.